Mapping the Corneal Sub-basal Nerve Plexus in Keratoconus by In Vivo Laser Scanning Confocal Microscopy

Dipika V. Patel and Charles N. J. McGhee

Purpose. To produce a two-dimensional reconstruction map of the living corneal sub-basal nerve plexus in keratoconus with in vivo confocal microscopy.

Methods. Four eyes of four subjects with keratoconus were examined by slit lamp biomicroscopy, Orbscan II slit-scanning elevation topography (Bausch & Lomb Surgical, Rochester, NY), and laser scanning in vivo confocal microscopy with the Heidelberg Retina Tomograph II, Rostock Corneal Module (Heidelberg Engineering, Heidelberg, Germany). Subjects were asked to fixate on targets arranged in a grid to enable in vivo confocal microscopy of the cornea in a wide range of positions.

Results. A mean of 402 ± 57 images were obtained for each cornea, to create confluent montages. The mean dimensions of the corneal areas mapped were 6.60 ± 0.70 mm horizontally and 5.91 ± 0.72 mm vertically. All corneas exhibited abnormal sub-basal nerve architecture compared with patterns previously observed in normal corneas. At the apex of the cone, a tortuous network of nerve fiber bundles was noted, many of which formed closed loops. At the topographic base of the cone, nerve fiber bundles appeared to follow the contour of the base, with many of the bundles running concentrically in this region. Central sub-basal nerve density was significantly lower in keratoconus corneas (10,478 ± 2,188 μm/mm^2) compared with normal corneas (21,668 ± 1,411μm/mm^2; Mann-Whitney; $P < 0.01$).

Conclusions. This is the first study to elucidate the overall distribution of sub-basal nerves in the living central to midperipheral human cornea in keratoconus, using laser scanning in vivo confocal microscopy. (*Invest Ophthalmol Vis Sci.* 2006; 47:1348–1351) DOI:10.1167/iovs.05-1217

Keratoconus is a noninflammatory disorder in which the cornea assumes a conical shape due to thinning and protrusion.[1] Classically, onset is at puberty, with progression until the third or fourth decade of life, when it usually arrests.[2] Clinically, this corneal ectasia leads to myopia and irregular astigmatism, and in severe cases, ruptures in Descemet's membrane may occur, resulting in corneal edema and scarring.[1] The pathophysiology of keratoconus has yet to be fully resolved, though there appears to be an underlying genetic predisposition.[3]

From the Department of Ophthalmology, Faculty of Medical and Health Sciences, University of Auckland, Auckland, New Zealand.

Supported in part by an unrestricted award from The Maurice and Phyllis Paykel Trust.

Submitted for publication September 13, 2005; revised November 3, 2005; accepted January 9, 2006.

Disclosure: **D.V. Patel**, None; **C.N.J. McGhee**, None

The publication costs of this article were defrayed in part by page charge payment. This article must therefore be marked "*advertisement*" in accordance with 18 U.S.C. §1734 solely to indicate this fact.

Corresponding author: Charles N. J. McGhee, Department of Ophthalmology, Private Bag 92019, University of Auckland, Auckland, New Zealand; c.mcghee@auckland.ac.nz.

The in vivo confocal microscope provides a unique opportunity for examination of the living human cornea at the cellular level. The noninvasive nature of this technique means that multiple examinations may be performed on the same tissue over time, and the induction of artifacts observed with ex vivo methods of examination are avoided. For these reasons, in vivo confocal microscopy has increasingly been used in the assessment of several inherited corneal diseases.[4] However, compared with ex vivo microscopy techniques, a current limitation is that tissue-staining techniques cannot be used in conjunction with in vivo confocal microscopy in human subjects, and the maximum resolution is in the region of 1 to 2 μm.

In a recent study, we used laser scanning in vivo confocal microscopy to elucidate the architecture of the living human corneal sub-basal nerve plexus for the first time.[5] The study revealed a radiating pattern of nerve fiber bundles converging toward an area approximately 1 to 2 mm inferior to the corneal apex in a whorl-like pattern. The purpose of the present study was to use these techniques to produce a two-dimensional reconstruction of the living human corneal sub-basal nerve plexus in keratoconus, with laser scanning in vivo confocal microscopy.

Methods

Four subjects with an established diagnosis of keratoconus were recruited for the study. Exclusion criteria were previous contact lens wear, history of ocular trauma or surgery, ocular disease other than keratoconus, and systemic disease that may affect the cornea. Two subjects were men and two were women (mean age, 44 ± 9 years).

All research protocols adhered to the tenets of the Declaration of Helsinki. Before enrollment, informed, written consent was obtained from all subjects after an explanation of the nature and possible consequences of the study. The protocol used was approved by the Auckland ethics committee.

Slit lamp biomicroscopy was performed on all eyes, and each subject exhibited one or more of the following clinical signs: central corneal stromal thinning, Fleisher's ring, Vogt's striae or Munson's sign. No eyes had signs of corneal hydrops or scarring. In all cases, slit-scanning elevation topography (Orbscan II; Bausch & Lomb Surgical, Rochester, NY) was performed to confirm the clinical diagnosis and to classify further the severity of keratoconus. The modified Rabinowitz-McDonnell test was used to confirm the diagnosis of keratoconus,[6] and the severity of keratoconus was classified according to the steepest reading on the keratometric map (mild, <45 D; moderate, 45–52 D; and severe, >52 D).

Laser scanning in vivo confocal microscopy was subsequently performed on all subjects (Heidelberg Retina Tomograph II, Rostock Corneal Module [RCM]; Heidelberg Engineering GmbH, Heidelberg, Germany). This microscope utilizes a 670-nm red wavelength diode laser source. It is a class 1 laser system and so, by definition, does not pose any ocular safety hazard. However, to guarantee the safety of the operator and subjects, the manufacturers have imposed a limit on the maximum period of exposure for patient and operator of 3000 seconds (50 minutes) in any single examination period. A 60× objective water-immersion lens with a numerical aperture of 0.9 (Olympus, Tokyo,

Investigative Ophthalmology & Visual Science, April 2006, Vol. 47, No. 4

TABLE 1. A Summary of the Data Obtained for Each Subject and Eye Examined

Subject	Age (y)	Eye Examined	Steepest Keratometry (D)	Topographic Severity Classification	Images Obtained	Images Used in Montage
A	53	OD	44.0	Mild	712	411
B	43	OD	49.4	Moderate	631	428
C	48	OD	49.2	Moderate	688	450
D	31	OS	55.0	Severe	597	321

Japan) and a working distance, relative to the applanating cap, of 0.0 to 3.0 mm was used. The dimensions of each image produced using this lens are 400 μm $\times$ 400 μm, and the manufacturers quote transverse resolution and optical section thickness as 2 and 4 μm, respectively. The RCM uses an entirely digital image capture system.

Eyes were anesthetized with a drop of 0.4% benoxinate hydrochloride (Chauvin Pharmaceuticals, Romford, UK). Viscotears (Carbomer 980, 0.2%; Novartis, Basel, Switzerland) was used as a coupling agent between the applanating lens cap and the cornea. During the examination, all subjects were asked to fixate on distance targets arranged in a grid pattern, as described previously.[5]

The cornea was scanned, using the device's "section mode" to obtain high-quality images of the sub-basal nerve plexus in each position. The section mode enables instantaneous imaging of a single area of the cornea at a desired depth. The overall examination took approximately 40 minutes to perform for each subject, including breaks every few minutes and a total in vivo confocal exposure time of less than 20 minutes. None of the subjects experienced any visual symptoms or corneal complications as a result of the examinations.

A software program (Freehand 10; Macromedia, San Francisco, CA) was used to arrange images from each eye into wide-field montages of the sub-basal nerve plexus. Sub-basal nerve density measurements were performed on the montage using a caliper tool (analySIS 3.1; Soft Imaging System, Münster, Germany). In all cases, a standard frame size of 0.8 $\times$ 0.8 mm (area, 0.64 mm^2) was selected. Nerve density was assessed in the region of the central cornea by measuring the total length of nerves per defined frame.

RESULTS

A mean of 657 $\pm$ 52 images were obtained from four eyes of four subjects (Table 1). All blurred, oblique, or duplicate images were discarded. Wide-field montages were thus created with a mean of 402 $\pm$ 57 images (Fig. 1b). The fewest images were used in the severe case of keratoconus, because of the movement of the subject's eyes during examination resulting in multiple oblique or blurred images. The mean dimensions of the corneal areas that were mapped were 6.60 $\pm$ 0.70 mm horizontally and 5.91 $\pm$ 0.72 mm vertically.

Using a tablet and pen (Wacom Co., Ltd., Japan), we performed electronic tracings of nerve fiber bundles on all the in vivo confocal montage images. This enabled the production of schematics of the sub-basal nerve plexus in all four subjects. These line schematics were subsequently superimposed (to scale) onto tangential keratometric maps obtained by Orbscan II slit-scanning elevation topography (Fig. 2). Regions of the line schematics corresponding to the corneal apex (as determined by saved charge-coupled device [CCD] camera images of the cornea taken from the temporal side during examination) were aligned with the topographic corneal apex.

In all subjects, sub-basal nerve fiber bundles exhibited abnormal configurations at the apex of the cone where the sub-basal nerve plexus appeared to consist of a tortuous network of nerve fiber bundles, many of which formed closed loops. At the topographic base of the cone, nerve fiber bundles appeared to follow the curvilinear contour of the base, with many of the bundles appearing to run concentrically with the cone in this region. Nerve fiber bundles in the region of the apex of the cone appeared to adopt oblique or horizontal orientations in keratoconus corneas. The mean central nerve density for subjects with keratoconus was 10,478 $\pm$ 2,188 μm/mm^2. The mean sub-basal nerve density for the corresponding central area in normal subjects has been reported, using an identical technique, as 21,668 $\pm$ 1,411 μm/mm^2.[5] The difference in nerve density between these two groups is statistically significant (Mann-Whitney; $P < 0.01$), although the sample size is small.

In two of the subjects, A and C, focal abnormalities in Bowman's layer were observed. These consisted of irregularly shaped, well defined, areas of hyperreflectivity containing mul-

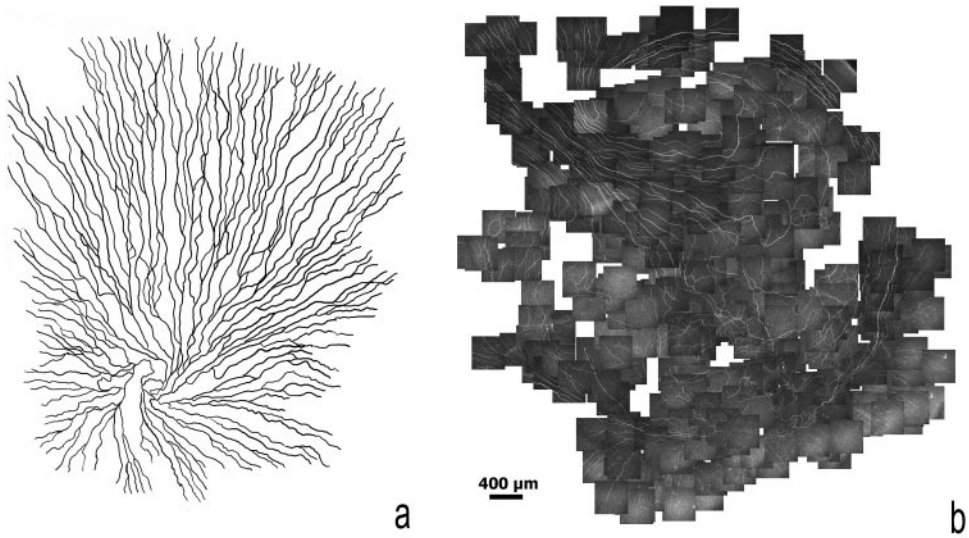

FIGURE 1. (**a**) Schematic showing the architecture of the normal human sub-basal nerve plexus. (**b**) A wide-field montage consisting of 428 images, depicting the architecture of the sub-basal nerve plexus in a case of moderate keratoconus in subject B.

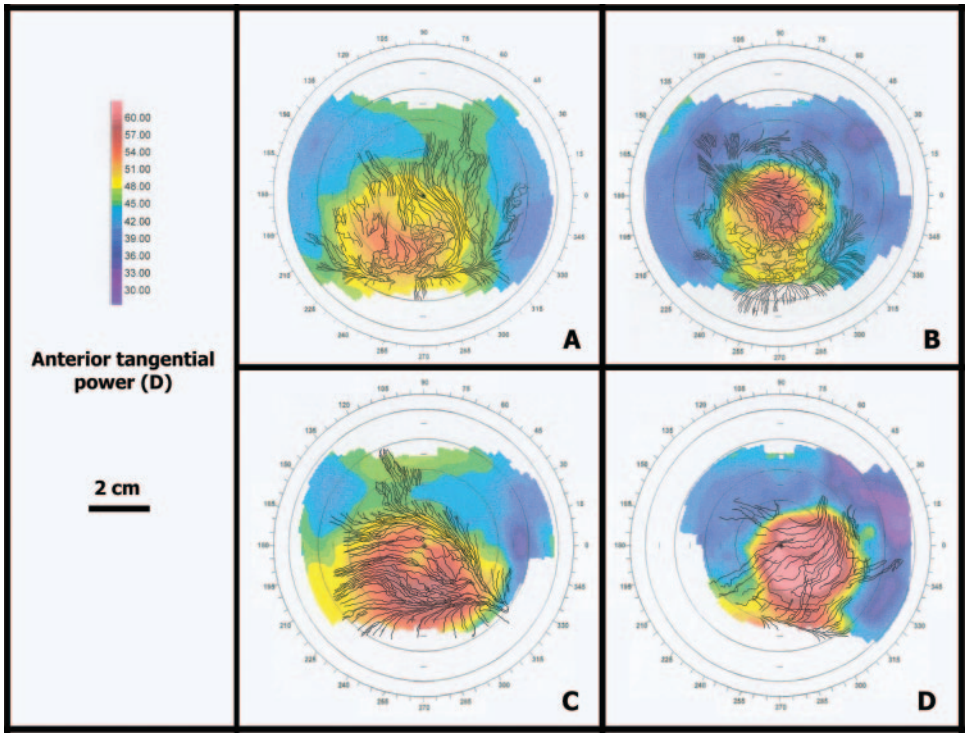

FIGURE 2. Electronic tracings of nerve fiber bundles provide schematics devoid of background data in the four subjects, labeled A, B, C, and D. These tracings are superimposed, to scale, onto the corresponding anterior tangential corneal topography maps.

tiple oval-shaped bright objects (Fig. 3). Dynamic scanning confirmed that these regions extended from the anterior stroma and did not extend into the corneal epithelium. They were observed in the region of the base of the cone, particularly inferiorly.

In the subject with severe keratoconus (D), some of the nerve fiber bundles appeared to terminate abruptly within the region of the cone (Fig. 4). These features were not observed in the mild or moderate cases of keratoconus.

DISCUSSION

The recent development of a technique for mapping the corneal sub-basal nerve plexus[5] opens up new avenues for the investigation of sub-basal nerves in health and disease.

This study is the first to map the architecture of the sub-basal nerve plexus in keratoconus and has demonstrated that keratoconus is associated with grossly abnormal sub-basal nerve morphology, even in mild keratoconus. As none of the subjects had a history of contact lens wear, previous ocular surgery or other disease involving the cornea, it is reasonable to conclude that the abnormal sub-basal nerve architecture observed is primarily related to keratoconus and its pathophysiology. In the present study, all the subjects with keratoconus exhibited abnormal sub-basal nerve architecture. The predominantly oblique and horizontal orientation of sub-basal nerve fibers at the apex, and the curvilinear orientation at the base of the cone differ markedly from the pattern of nerve fibers radiating toward an inferocentral whorl-like region that is observed in the normal cornea.

In the present study, alignment of the line schematics with tangential keratometric maps is a novel method of determining the relationships between sub-basal nerve architecture and corneal topography. However, this technique is limited by the fact that, although the live CCD camera is useful for localizing the approximate area of the cornea under examination, it is not sufficiently accurate to enable determination of the exact point location of the corneal apex to better than approximately 1.00 mm.

To date, there are only five studies in the published literature in which in vivo confocal microscopy was used specifically to investigate the cornea in keratoconus.[7–11] These studies have largely concentrated on evaluation of the central

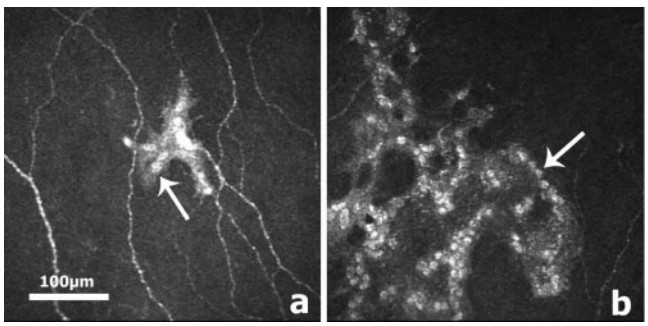

FIGURE 3. Focal areas of hyperreflectivity at the level of Bowman's layer at the topographic base of the cone in subject C, (**a**) superiorly and (**b**) inferotemporally.

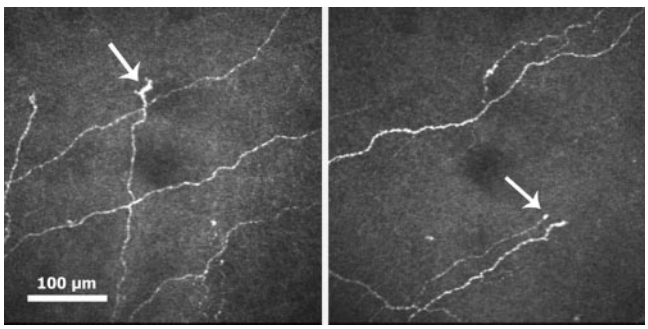

FIGURE 4. Apparent abrupt terminations of sub-basal nerve fiber bundles within the region of the cone in severe keratoconus in subject D.

cornea and have provided useful insights into cellular changes occurring at the level of the corneal epithelium, stroma, and endothelium. However, there are few in vivo data regarding alterations in the sub-basal nerve plexus. In a recent qualitative in vivo confocal microscopy study, sub-basal nerve fibers were noted to run in and out of the plane of the field of view in the central cornea.[7]

A role for the corneal nerves in the pathophysiology of keratoconus has been suggested. Clinical support for this theory also comes from a case of unilateral progression of keratoconus after fifth nerve palsy.[12] In a transmission electron microscopy study of keratoconus corneal discs removed at penetrating keratoplasty, Teng[13] noted nerve fibers within the corneal epithelium showed signs of moderate degeneration, with break-up of the nerve fiber membrane and liquefaction of neurofibrils. Brookes et al.[14] provided evidence that the destructive process in keratoconus involved the nerves or their associated Schwann cells, which express proteolytic enzymes (cathepsin B and G) more extensively in corneas affected by keratoconus than in normal corneas. The present study confirms that the architecture of the sub-basal nerve plexus is altered in keratoconus and provides quantitative evidence of a significant reduction in sub-basal nerve density compared with normal. The pattern and density of the sub-basal nerve plexus is altered in the keratoconus disease process, even during the early stages, although it remains unclear whether these changes are a causative factor in, or occur secondary to, the structural changes in the cornea. It is also unclear how these changes relate to the paradoxical apparent prominence of stromal corneal nerves in subjects with keratoconus.[1]

The observation that sub-basal nerve fiber bundles exhibit the most abnormal configurations at the apex of the cone correlates well with ex vivo studies demonstrating that the greatest destruction of normal corneal architecture occurs at the apex of the cone and that there is a gradient of diminishing damage toward the periphery.[14]

The multiple oval shaped hyperreflective objects noted within focal hyperreflective regions at the level of Bowman's layer (Fig. 3) most likely represent keratocyte nuclei as they were observed to extend from the anterior stroma and exhibit similar morphologies. This observation correlates well with features noted by Sherwin et al.[15] in their unique ex vivo study of the peripheral keratoconus cone. In this study, we noted that in the peripheral cone keratocyte cell processes traversed Bowman's layer, thus linking the stroma to the corneal epithelium. Cellular material occupied localized fractures in the normally acellular Bowman's layer. Several studies have reported similar breaks in Bowman's layer in the keratoconus corneal apex,[16–19] although this feature was noted only in the region of the topographic base of the cone in our study. This may be attributed to the fact that investigators in ex vivo studies use corneal tissue obtained at penetrating keratoplasty, thus only sampling the very severe end of the disease spectrum. The use of in vivo confocal microscopy in our study has enabled examination of the cornea through a range of disease severity.

The apparent abrupt termination of sub-basal nerve fiber bundles observed within the cone of the severe case of keratoconus under study has not previously been reported. These regions may represent sites of perforation of nerve fiber bundles through Bowman's layer, and nerves crossing Bowman's layer are known to be closely associated with both keratocyte and epithelial nuclei.[14] Postulated perforation sites have been reported in the normal sub-basal nerve plexus imaged by in vivo confocal microscopy[5]; however, these were most commonly observed in the midperipheral cornea and were associated with bright, irregularly shaped areas, 20 to 40 μm in diameter. An alternative explanation is that the features described represent true nerve fiber bundle termination points. This may correspond to an extension of the nerve degeneration that has been observed in epithelial nerve fibers.[13]

We report the first study to elucidate the distribution of sub-basal nerves in the living human cornea with keratoconus and to correlate the two-dimensional distribution with computerized corneal topography. Although this pilot study is limited by the small number of subjects, it provides interesting new data regarding the architecture of the corneal sub-basal nerve plexus in keratoconus and provides strong evidence for the involvement of these nerves in the disease process. Future studies may be directed at examining subjects with keratoconus over time to observe whether changes in sub-basal nerve architecture precede or follow progression of the disease. It would also be of interest to investigate the effects of contact lens wear on the configuration of sub-basal nerves in patients with keratoconus.

References

1. Krachmer JH, Feder RS, Belin MW. Keratoconus and related noninflammatory corneal thinning disorders. *Surv Ophthalmol*. 1984; 28:293–322.
2. Rabinowitz YS. Keratoconus. *Surv Ophthalmol*. 1998;42:297–319.
3. Edwards M, McGhee CN, Dean S. The genetics of keratoconus. *Clin Exp Ophthalmol*. 2001;29:345–351.
4. Vincent AL, Patel DV, McGhee CN. Inherited corneal disease: the evolving molecular, genetic and imaging revolution. *Clin Exp Ophthalmol*. 2005;33:303–316.
5. Patel DV, McGhee CNJ. Mapping of the normal human corneal sub-basal nerve plexus by in vivo laser scanning confocal microscopy. *Invest Ophthalmol Vis Sci.* 2005;46:4485–4488.
6. Maeda N, Klyce SD, Smolek MK. Comparison of methods for detecting keratoconus using videokeratography. *Arch Ophthalmol*. 1995;113:870–874.
7. Hollingsworth JG, Bonshek RE, Efron N. Correlation of the appearance of the keratoconic cornea in vivo by confocal microscopy and in vitro by light microscopy. *Cornea*. 2005;24:397–405.
8. Hollingsworth JG, Efron N. Observations of banding patterns (Vogt striae) in keratoconus: a confocal microscopy study. *Cornea*. 2005;24:162–166.
9. Hollingsworth JG, Efron N, Tullo AB. In vivo corneal confocal microscopy in keratoconus. *Ophthalmic Physiol Opt*. 2005;25: 254–260.
10. Erie JC, Patel SV, McLaren JW, et al. Keratocyte density in keratoconus: a confocal microscopy study. *Am J Ophthalmol*. 2002;134:689–695.
11. Somodi S, Hahnel C, Slowik C, et al. Confocal in vivo microscopy and confocal laser-scanning fluorescence microscopy in keratoconus [in German]. *Ger J Ophthalmol*. 1996;5:518–525.
12. Ruddle JB, Mackey DA, Downie NA. Clinical progression of keratoconus following a Vth nerve palsy. *Clin Exp Ophthalmol*. 2003; 31:363–365.
13. Teng CC. Electron microscopy study of the pathology of keratoconus. *Am J Ophthalmol*. 1963;55:18–47.
14. Brookes NH, Loh IP, Clover GM, et al. Involvement of corneal nerves in the progression of keratoconus. *Exp Eye Res*. 2003;77: 515–524.
15. Sherwin T, Brookes NH, Loh IP, et al. Cellular incursion into Bowman's membrane in the peripheral cone of the keratoconic cornea. *Exp Eye Res*. 2002;74:473–482.
16. Chi HH, Katzin HM, Teng CC. Histopathology of keratoconus. *Am J Ophthalmol*. 1956;42:847–860.
17. Sawaguchi S, Fukuchi T, Abe H, et al. Three-dimensional scanning electron microscopic study of keratoconus corneas. *Arch Ophthalmol*. 1998;116:62–68.
18. Kaas-Hansen M. The histopathological changes of keratoconus. *Acta Ophthalmol*. 1993;71:411–414.
19. Scroggs MW, Proia AD. Histopathological variation in keratoconus. *Cornea*. 1992;11:553–559.